Netherlands Journal of Geosciences / Geologie en Mijnbouw 82 (1): 19-30 (2003)

Radionuclide transport in clay during climate change

A.F.B. Wildenborg[1], B. Orlic[1], J.F. Thimus[2], G. de Lange[1], S. de Cock[2], C.S. de Leeuw[1,4] & E.J.M. Veling[3]

[1] Netherlands Institute of Applied Geoscience TNO – National Geological Survey, P.O. Box 80015, 3508 TA Utrecht, the Netherlands
[2] Université Catholique de Louvain, Place du Levant 1, B-1348 Louvain-la-Neuve, Belgium
[3] Technische Universiteit Delft, P.O. Box 5048, 2600 GA Delft, the Netherlands
[4] TotalFinaElf, P.O. Box 93.280, 2509 AG Den Haag, the Netherlands

Manuscript received: March 2002; accepted: November 2002

Abstract

The Dutch national research programme into the feasibility of retrievable storage of radioactive waste (CORA Programme Phase I; CORA: Comité Opslag Radioactief Afval = Committee on Radioactive Waste Disposal) examined the suitability of Tertiary clay deposits for such storage. Long-term isolation – up to 1 million years – of high-level radioactive waste under varying conditions is essential. A key concern is the hydro-mechanical response of the clay deposits in which radioactive waste might possibly be stored, in particular during glacial climate conditions as has happened repeatedly in the Netherlands during the Pleistocene. To evaluate this possibility hydro-mechanical computer simulations and mechanical laboratory experiments have been performed to analyse the effects of glacial loading by a thousand-metre-thick ice sheet on the permeability characteristics, fluid flow rates and the associated migration of radio-nuclides both within and out of Tertiary clays.
Glacial loading causes the expulsion of pore water from deeply buried clay deposits into adjoining aquifers. The rates and duration of the consolidation-driven outflow of water from the clay deposit, are very sensitive to the permeability of the clay and the dynamics of the advancing ice sheet. The maximum outflow rate of pore water is 1 mm per year. This rate is approximately three times faster than the flow rate of water in clay prior to ice loading. These preliminary simulation studies also indicate that cyclic loading can result in more rapid migration of radio-nuclides in clays. In clay deposits that are covered by a thick ice sheet, the contribution of dispersed transport relative to the total transport by diffusion amounts to 14%, assuming that there is no absorption of radio-nuclides by the clays and a longitudinal dispersivity of 50 m.

Keywords: Clay, glaciation, hydro-mechanical modelling, mechanical experiments, radionuclide transport

Introduction

One of the key themes in the Dutch R&D Programme CORA (= Comité Opslag Radioactief Afval = Committee on Radioactive Waste Disposal) Phase 1 (1996-2000; CORA Cie, 2001; Hageman & Van de Vate, in press) was an evaluation of retrievable disposal of radioactive waste in Tertiary clay deposits. For a limited period after placing the waste into a repository, retrievability should be guaranteed. After that period, the geological barriers should be capable of effectively isolating the waste from the biosphere. This paper presents an overview of one of the projects that are part of the CORA R&D Programme. This project focused on the geological stability of clay deposits in the medium-long term, i.e. tens to hundreds of thousands of years. During this type of period, climate changes related to glaciation may have a significant impact on the subsurface (TRACTOR; Wildenborg et al., 2000).

Under present-day climatic conditions, flow of groundwater and migration of radio-nuclides in clay deposits occurs at a very slow rate. Diffusion is the main migration mechanism in intact clay deposits, i.e. clay that is not damaged by faults or fractures. If, however, north-western Europe, including the Nether-

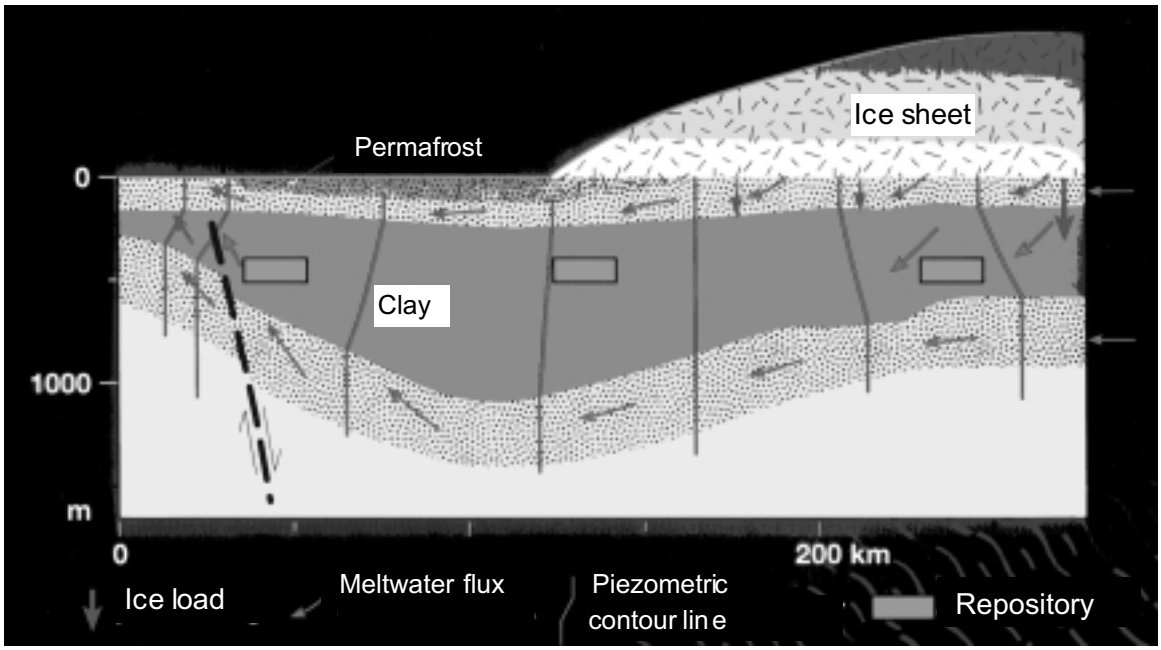

Fig. 1. Concept used for groundwater-flow modelling during ice loading and production of melt water underneath the ice cap.

lands, were once again to experience a glaciation, and become covered by ice, the present permeability characteristics might change (Fig. 1).

Clay has a very high water-bearing capacity and is very compressible. Mechanical loading by an ice cap could force water that might be contaminated by radio-nuclides out of the clay (compaction-driven outflow). As a result, migration of radio-nuclides to the shallow groundwater system could be accelerated.

In addition to mechanical loading, melt water from under the ice cap might infiltrate into the clay, causing an increase in water pressure and water-pressure gradient, as shown by research carried out at the University of Edinburgh, the Geological Survey of the Netherlands – RGD and the National Institute for Public Health and the Environment – RIVM (Boulton & Curle, 1997). The mechanical and hydraulic pressures generated by the ice cover are correlated. Depending on the three-dimensional architecture of the subsurface, the increase in pressure results in outflow of compaction water derived from the clay and/or in water derived from the ice cap percolating the host rock.

A complicating factor is the presence of permafrost. Most of the soils in front of the ice cap and also partly underneath it will be permanently frozen, isolating the shallow groundwater system from the biosphere. In permafrost soil, water cannot flow; this increases the length of the migration path to the biosphere of any radio-nuclides present in the outflow water. The presence of permafrost, however, also reduces the domain of shallow groundwater flow and therefore causes the flow rate in the shallow aquifer system to increase. Hydro-mechanical computer simulations of this coupled system were performed in order to quantify its effects on the migration of radio-nuclides.

Approach

A hydro-mechanical numerical model based on the finite-element package DIANA (2000) was used to simulate the effect of ice loading on the mechanical behaviour of the subsurface and the flow of groundwater. Compression and consolidation of the clays as a result of the weight of the ice and the groundwater flow driven by hydraulic gradients are simulated as fully coupled processes in DIANA. The required boundary conditions have been derived from a large-scale flow model AQ-FEM (i.e., a supra-regional model), which was used previously to simulate the impact of an ice cap on the groundwater system (Fig. 2).

The model is described in detail in a number of publications (Van Weert et al., 1997; Boulton & Curle, 1997). The hydro-mechanical calculations were done in two phases: The initial, fairly simple, model was used to evaluate a large number of potential situations. The information acquired from these initial calculations was then used to build a more detailed hydro-mechanical model. The resulting flow rates were subsequently used to model radionuclide transport using METROPOL-4 (Sauter et al., 1993).

In order to quantify the effects of ice loading on deeper clay deposits in the subsurface of the Netherlands, all soil-mechanical parameters have to be

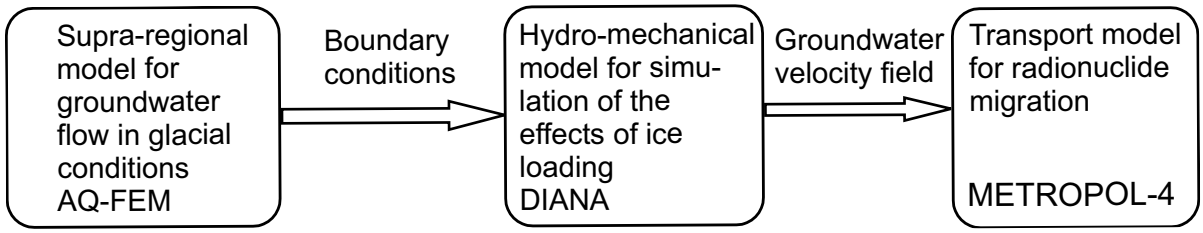

Fig. 2. Relationship between the hydro-mechanical model and the other models used in the study.

known. Input data for this modelling exercise were partly derived from the detailed site-characterisation studies that were performed in the Belgian Underground Research Laboratory located in the Boom Clay at Mol. Additional mechanical laboratory experiments were carried out to enable extrapolation of the Belgian data to the Boom Clay (Rupel Clay Member) in the Netherlands at depths of 500 m or more. These experiments focused on consolidation characteristics, permeability, strength and deformability of the clay. The material used for the experiments came mainly from the Rupel Clay Member, which occurs at various depths in Belgium and the Netherlands.

Mechanical experiments

Mechanical experiments were performed to characterise the mechanical properties of Tertiary clay, and of the Rupel Clay Member in particular. The experiments yielded information on the consolidation rate of clay as a function of the applied stress. Two types of mechanical loading experiments were performed: the uniaxial consolidation test (oedometer test) and the triaxial cell test.

The triaxial cell test involves encasing a soil sample in an impervious membrane, confining it to a desired initial state of stress and subsequently applying an increasing axial stress until the material fails. This type of test can be used to predict the parameters cohesion, friction angle and shear modulus. The oedometer test is a type of one-dimensional consolidation test, used for determining the compaction and swelling characteristics of the soil sample, including its vertical permeability.

Soil samples from six different depths from four locations in Belgium as well as from one location in the Netherlands were used. The experiments intended to study the effects of ice loading focused on analysing the material from the greatest depth, in one core taken in the Netherlands and one in Belgium. All but one of the samples concern the Rupel Clay Member. The sample from the greatest depth, cored at a depth of approximately 562 metres, belongs to the Asse Member, immediately underlying the Rupel Clay Member. All clay samples comprise a mixture of the minerals smectite, illite and kaolinite. The clay sample from the Asse Member contains approximately 50% smectite; the smectite content of the Rupel Clay Member samples ranges from 30% to 50%.

The stresses applied in the mechanical experiments were correlated with the depths from where the samples were taken and the additional maximum loading that a potential future glacial cover might cause (Table 1). The apparatus available for the triaxial tests did not permit confining stresses over 10 MPa.

Triaxial cell tests

Most triaxial cell tests exhibit normally consolidated behaviour for the clay material. This is as expected for the experiments using samples from the Blija core and case 5 of the Weelde core, but in all other experiments the applied stress is lower than the pre-consolidation stress. This unexpected normally consolidated behaviour is attributed to disturbance of the original condition of the samples. During the long period be-

Table 1. Summary of triaxial cell tests and oedometer tests including stress levels.

Type of experiment/ sampling site	Depth range (m)	Effective stress level (MPa)
Triaxial/Weelde (B)		
Case 1 (3 samples)	313 - 314	3.1 - 6.3
Case 2 (3 samples)	314 - 315	2.3 - 4.1
Case 3 (3 samples)	314 - 315	3.6 - 6.4
Case 5 (3 samples)	314 - 315	5.4 - 9.4
Triaxial/Blija (NL)		
Case 1 (3 samples)	454 - 455	4.6 - 9.2
Case 4 (3 samples)	561 - 562	4.8 - 9.8
Oedometer/Weelde (B)		
Case 1 (1 sample)	313 - 314	0.6 - 9.0
Case 2 (1 sample)	314 - 315	0.6 - 12.0
Case 3 (1 sample)	313 - 314	0.6 - 16.0
Case 4 (1 sample)	313 - 314	0.6 - 19.0
Oedometer/Blija (NL)		
Case 1 (1 sample)	453 - 454	0.6 - 20.0
Case 2 (1 sample)	561 - 562	0.6 - 20.0

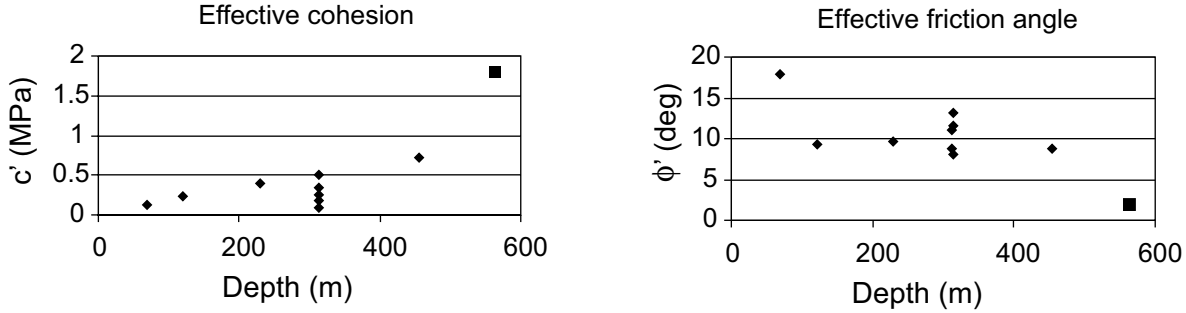

Fig. 3. Results of the triaxial cell test; the clay sample from the deepest level is from the Asse Member(■); all others are Rupel Clay Member samples (◆).

tween extraction from the sampling tubes and the actual experiments, the clay samples probably experienced some swelling.

The results of the triaxial cell test suggest an increase in cohesion and shear modulus with depth and suggest a decrease in friction angle with depth (see also Fig. 3).

The depth relationship suggests that the clay would behave more plastically with depth. This is corroborated by the results of mechanical test on the London Clay (Bishop et al., 1965). We have too few observations, however, to prove this relationship. Also, not all samples came from the same geological unit. The mechanical characteristics of clay from a certain depth are variable, which is shown by the analyses for the depth intervals from 313 to 314 metres in the Weelde core. The variation in characteristics is very comparable with previously published results on experiments on the Rupel Clay Member in Belgium.

In view of the variation in results for the Weelde core, the number of experiments on material from the Dutch core is too small to formulate absolute conclusions on the parameter values to be used. Extremely high plastic behaviour was observed in the clay samples from the Asse Member. This will need to be verified by follow-up studies.

Generic strength parameters for the Rupel Clay Member can, however, be determined by plotting all shear-strength values against the average effective stress at failure in a so-called p'-q diagram (Fig. 4), yielding a Mohr-Coulomb failure envelope.

Fig. 4 also includes data obtained for samples from the Pleistocene Eem Clay in Amsterdam. The failure envelope found this way is comparable to that found for the Tertiary London Clay (Bishop et al. 1965). In both clays a decrease in friction angle with increasing effective stress was also observed: from an initial value of 30° at low stresses to approximately 10° at an effec-

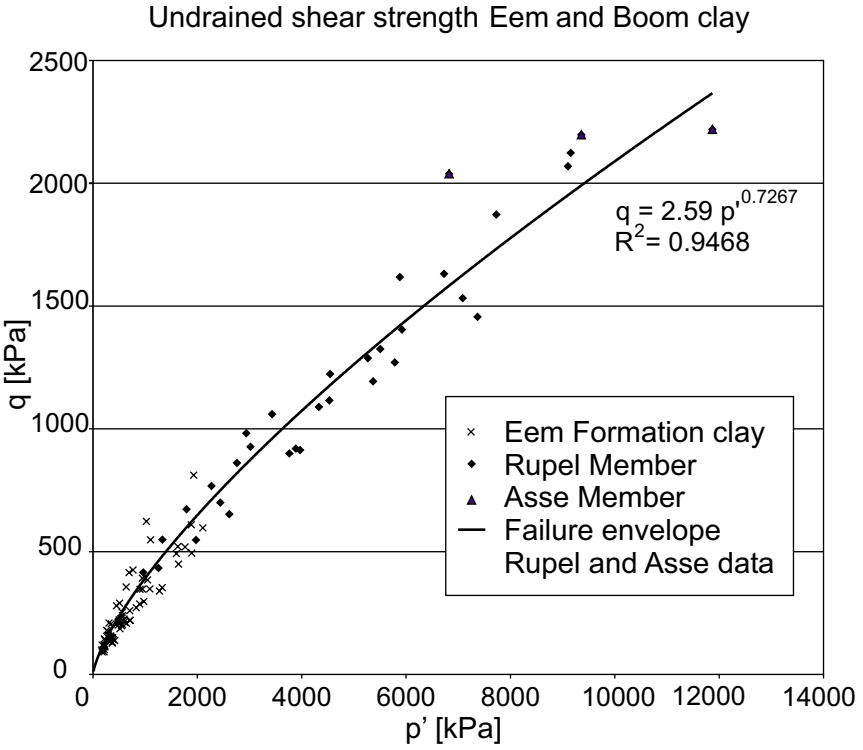

Fig. 4. Relationship between average effective stress p' and undrained shear stress q obtained from all tests on the Rupel and Asse Member clays, as well as test results for the Eem clay in Amsterdam. The exponential regression line is a good approximation of the failure envelope.

tive stress of 6 MPa. The behaviour we observed may therefore be generally applicable to Tertiary clays. This will have to be confirmed by follow-up studies.

Oedometer tests

The oedometer tests show good reproducibility of the results of the individual Weelde and Blija material (Fig. 5). The loading and decompression sections in the curves of the Belgian samples compare well. In case of the Dutch samples, higher compressive stresses are required to achieve the same amount of compaction.

Closer scrutiny of the stress curves enables a subdivision into three phases:

– an initial phase up to approximately 1.5 MPa,
– a second phase up to approximately 6–7 MPa for Weelde and 7–8 MPa for Blija and
– a third phase all the way to maximum applied stress.

The vertical stress at the end of the second loading phase has been interpreted as corresponding to the actual pre-consolidation stress. The value of 6 to 7 MPa for Weelde agrees well with the prognosis made on the basis of observations in shallow clay deposits underneath the Westerschelde (p'c = 350 + 20*z (kPa); z = depth in metres). The related over-consolidation ratio (ratio of pre-consolidation stress and in-situ stress) is 1.9 to 2.2. The steep gradient in phase 2 is attributed to disturbance of the sampling material (for an explanation see the Weelde triaxial cell tests described above). This is corroborated by the fact that the loading curves for Weelde are virtually identical to the Intrinsic Compression Line (ICL), which is the virgin loading curve for completely reworked clay (Burland, 1990).

The over-consolidation ratio for the Blija samples is between 1.3 and 1.8. This is less than predicted on the basis of observations in the shallow domain. The loading curves for Blija approach the Sedimentary Compression Line (SCL). This means that the clay samples behave similarly to clay compacting under natural geological conditions.

The observed over-consolidation of Tertiary clays that are millions of years old are attributed to diagenesis and creep processes (aging) as well as to the fact that in the geological past, the clay was subjected to a higher loading than it is at present. It is very difficult to distinguish between the effects of aging and of overloading.

Fig. 5 shows the pre-consolidation stresses and the effective stress caused by a thousand-meter-thick ice cover. Such an extreme load would result in further consolidation of the clay. The actual effective stress caused by the ice could be less because of the presence of melt water underneath the ice cap. The melt water would increase the water pressure and therefore decrease the effective stress. The oedometer tests yielded input parameters for the Cam-Clay material model, i.e., the compression index λ and the swelling index κ (Table 2).

The permeability values (K) for the Rupel Clay Member underneath the Westerschelde were extrapolated to greater depths and yielded values ranging

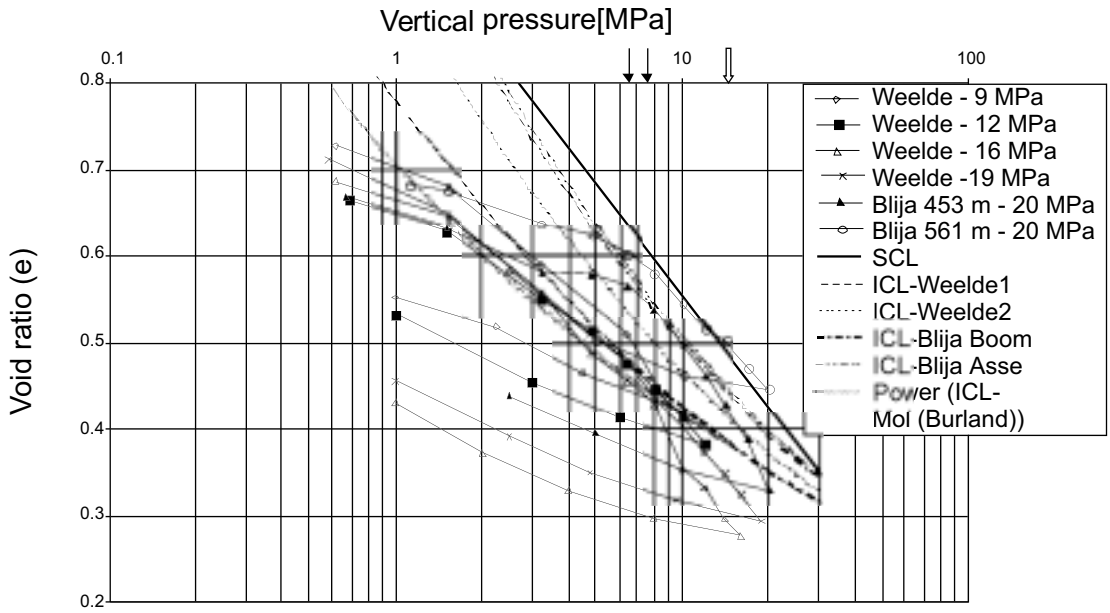

Fig. 5. Results of oedometer tests – void ratio e versus vertical stress; ICL = Intrinsic Compression Line, which approaches the theoretical compression of a completely reworked clay sequence in the laboratory (Burland, 1990); SCL = Sedimentary Compression Line, which approaches compression of clay under natural geological conditions; solid arrow = pre-consolidation stress, open arrow = effective in-situ stress including a load of a 1000-metre-thick ice cover.

Table 2. Cam-Clay parameters κ (swelling index) and λ (compression index) derived from the oedometer tests; values for κ and λ were also based on an isotropic triaxial cell test (TRUCK-II). The values found in the latter test were used for hydromechancial modelling. p'c = pre-consolidation stress.

Location/ type of test	Depth (m)	Maximum loading [MPa]	κ [-]	λ [-]	P'c [MPa]
Weelde					
oedometer	313	9	0.06	0.24	6.4
oedometer		12	0.06	0.16	6.5
oedometer		16	0.06	0.21	8.0
oedometer		19	0.06	0.16	6.4
Blija					
oedometer	453	20		0.20	7.4
oedometer	561	20		0.14	7.5
triaxial	478	–	0.02	0.12	6.9

from 1.2 x 10^{-11} m/s to 5.4 x 10^{-15} m/s. The permeability values derived from the oedometer experiments range from 1.1 x 10^{-13} m/s to 7.6 x 10^{-14} m/s, which falls within the range extrapolated from the Westerschelde data. The void ratios (e) derived from the Weelde and Blija experiments exceed the prognosis made on the basis of the Westerschelde observations. Obviously, the relationship between void ratio (e) and permeability value (K) cannot be merely extrapolated from shallow data to greater depths.

Hydro-mechanical modelling

The hydro-mechanical modelling study of the impact of ice loading on Tertiary clay, described in detail in Orlic & Wildenborg (2001), was done in two phases. During the first phase, a relatively simple model was used for a preliminary study into the impact of ice loading on clay. The knowledge thus acquired was used to develop a more detailed model for the second phase, taking into account the newly available laboratory results.

The relatively simple calculations assumed a 2D spatial model, representing a typical cross-section of the subsurface of the Netherlands with a length of 10 km and extending to 1200 metres deep. In order to perform the calculations, a number of boundary conditions had to be established (see Fig. 6). More than ten scenarios were defined to test the responses of the model to variations in input parameters and boundary conditions (Table 3).

In all scenarios, the maximum thickness of the ice cap was thousand metres. The length of time that the ice moves across the model area ranges from 50 years to 3000 years and the total duration of the ice loading ranges from 600 to 6000 years.

The Mohr-Coulomb material model (ideal elastic – perfectly plastic model) was used to simulate the hydro-mechanical behaviour of the Tertiary deposits. The parameters for the Mohr-Coulomb model were obtained by compilation of data available in existing reports (Wildenborg et al., 2000).

For the second phase – the more detailed simula-

Table 3. Range of hydro-mechanical parameters and boundary conditions used in the glacial compression scenarios calculated in the first phase of the simulations.

Parameter	Value
Hydraulic gradient (-) (for lateral inflow boundary)	$i=5x10^{-4}$ $i=4x10^{-3}$ $i=8x10^{-3}$
Geomechanical parameters Rupel Clay Member (c=cohesion; ϕ =friction angle)	c=0.1 MPa, ϕ =20° c=0.2 MPa, ϕ =27°
Hydraulic conductivity Rupel Clay Member	$K=1x10^{-10}$ m/s $K=1x10^{-9}$ m/s

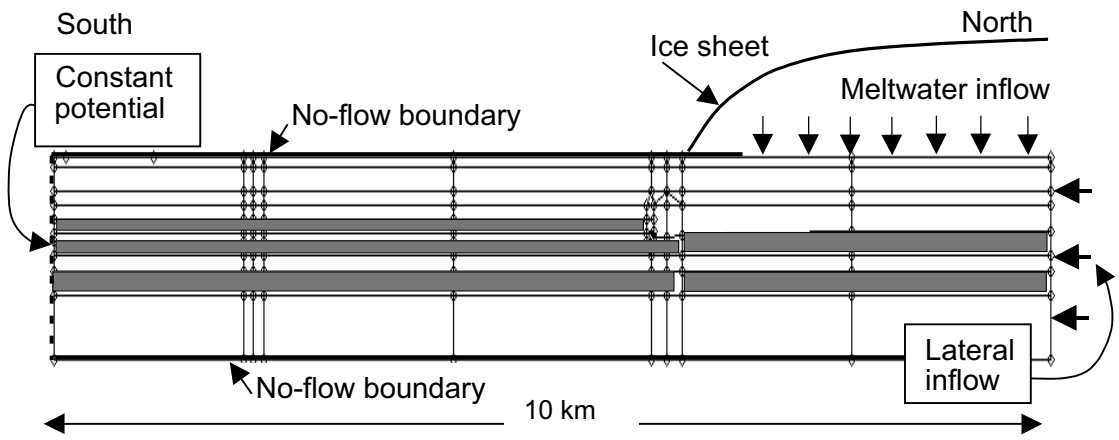

Fig. 6. Typical geo-hydrological boundary conditions.

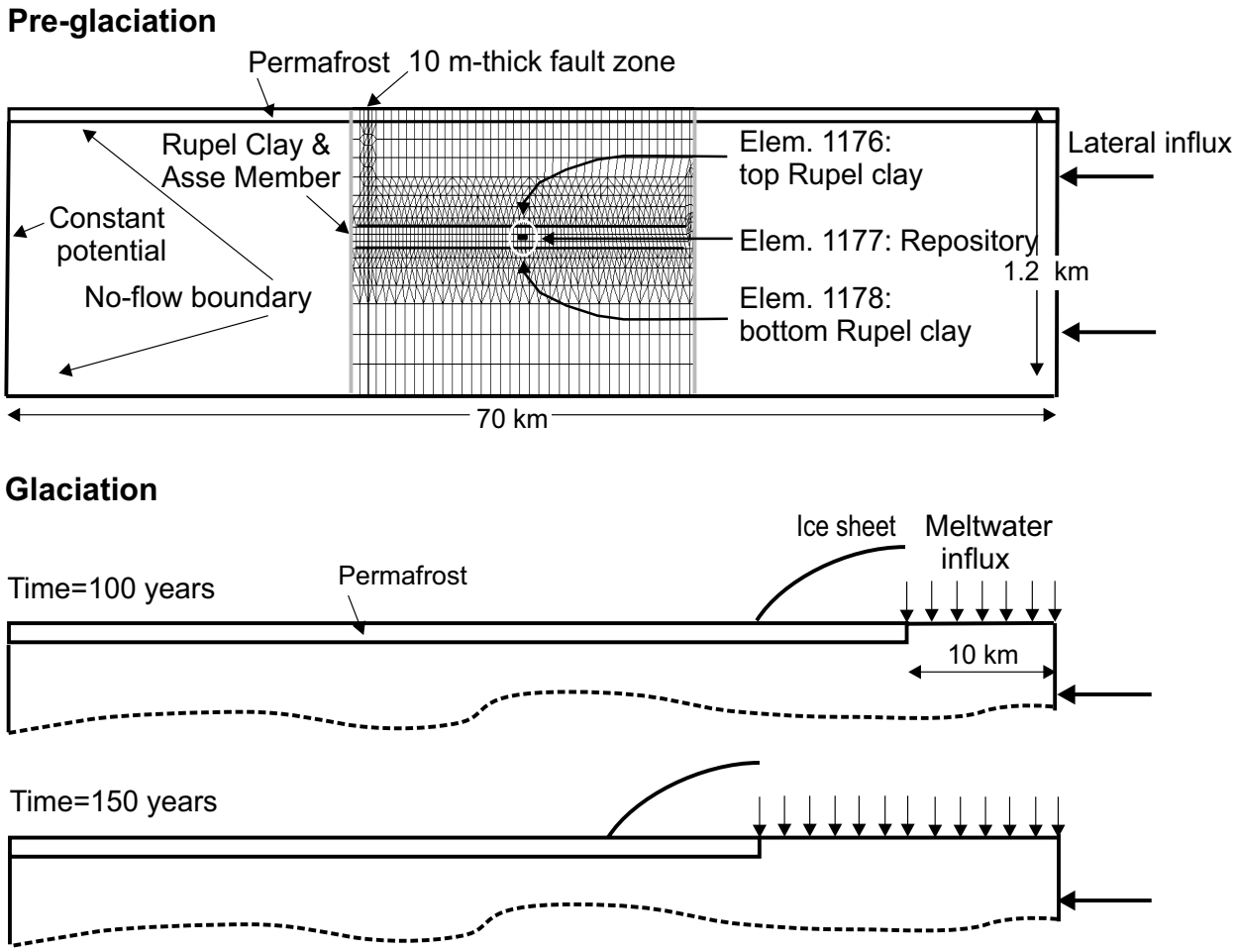

Fig. 7. Hydro-mechanical finite-element model used for simulations. The repository is assumed to be located in the middle of element 1177.

tions – the length of the geometric model was increased from 10 km to 70 km (Fig. 7).

This length corresponds better to the dimensions of a potential ice cap and the hydraulic boundary conditions associated with such an ice cap. The spatial model includes a 10-metre-wide fault zone. The geo-hydrological boundary conditions are largely identical to the boundary conditions used for the first phase of calculations.

Four characteristic scenarios were calculated (Table 4). In the first three scenarios different constitutive models were used for the clay: a purely elastic

Table 4. Range of constitutive models and parameters for the Rupel Clay and the clay of the Asse Member used in the ice-loading scenarios calculated in the second phase of simulations.

Parameter	**Value**			
Hydraulic gradient (-) (for lateral inflow boundary)			$i = 8x10^{-3}$	
Constitutive model Rupel Clay Member	Elastic	Mohr-Coulomb	Mod. Cam-Clay	Mod. Cam-Clay (loading/unloading)
	–	$\phi = 15°$	$\phi = 20°$	$\phi = 20°$
Geomechanical parameters Rupel Clay Member (ϕ=friction angle, c=cohesion; λ=compression index, κ=swelling index, p'c=pre-consolidation stress)	–	c= 0.2 MPa	$\lambda = 0.12$; $\kappa = 0.02$; p'c = 10.4 MPa	
Hydraulic conductivity Rupel Clay Member			$K = 3x10^{-12}$ m/s	

model, with an elasticity modulus of E=520 MPa; a Mohr-Coulomb model and a Modified Cam-Clay model. In these scenarios the ice cap moves across the entire modelled area in 350 years and the total modelled period of loading lasts 20,000 years. In the fourth scenario the parameters for the clay were the same as in the third case. Cyclic loading of the model by the ice was applied here, with two loading and two unloading cycles.

In all scenarios the Mohr-Coulomb material model was used for other geological deposits, except for the clay. The values used for the friction angle were considerably lower than in the first simulation phase. The same applies to the permeability values. The simulated flow rate was used as input for the calculations of the radionuclide transport.

Simple simulation using the Mohr-Coulomb material model

In case of a fast to moderately fast advancing ice sheet, the flow pattern in the clay is governed mainly by consolidation of the clay. Groundwater flows out of the clay body, both at the top and the bottom. The vertical outflow rate of water from the Rupel Clay Member and the Asse Member clay increases to 2 cm per year for a permeability of $1x10^{-10}$ m/s (Fig. 8).

However, if the ice sheet advances more slowly, the effects of consolidation-driven flow in the clay are less pronounced and upward flow in the clay will prevail.

The impact of regional upward flow through the clay during ice loading is more noticeable at higher permeability values of the clays (K = $1x10^{-9}$ m/s). Higher clay permeability, moreover, causes a higher maximum flux and more rapid dissipation of the overpressures in the clay. The clay undergoes elastic deformation while the ice sheet moves across the model area. If the ice front advances faster, the clay does undergo plastic deformation.

More detailed simulation using the Mohr-Coulomb and the Cam-Clay material models

In clay that is not loaded by an ice sheet, the typical flow rate of groundwater ranges between 10^{-6} to $4x10^{-7}$ metres per year. In the model used for glacial conditions, without an ice cover, drainage occurs through a permeable fault zone in the deeper Mesozoic aquifer, resulting in a decrease in pore pressure in the aquifer. The water in the Mesozoic aquifer flows towards the fault from both sides. Upon reaching the fault, the water starts to flow upward through the fault zone until it reaches the shallow aquifer. There, the flow is no longer confined and the water spreads into the shallow aquifer, away from the fault.
The pressure caused by ice loading is transmitted to the underlying sediment with a time delay. By the time the ice has covered the entire model area, after three hundred and fifty years, approximately half the stress caused by the ice will have been transmitted to the sediment. Most of the stress caused by ice loading is then still absorbed by pore water.

Depending on the assumed permeability of the clay and the material model used, the delay is several hundreds of years to over twenty thousand years. By the end of the simulation, the effective stress will have increased by the maximum load exerted by the ice cap and the pore-water pressure will have returned to the initial values.

Evolution of the stress and the pore-water flow rate in the Rupel Clay Member and the clay of the Asse Member during glaciation are shown in Figs 9, 10 & 11 for three calculated scenarios. A change in slope of the effective stress paths shown in Figs 9a to 11a marks the transition from elastic to plastic deformation of the clay.

The most complex shape of the stress path can be observed in the case of cyclic loading and unloading by the ice, when a hysteresis in the stress path occurs

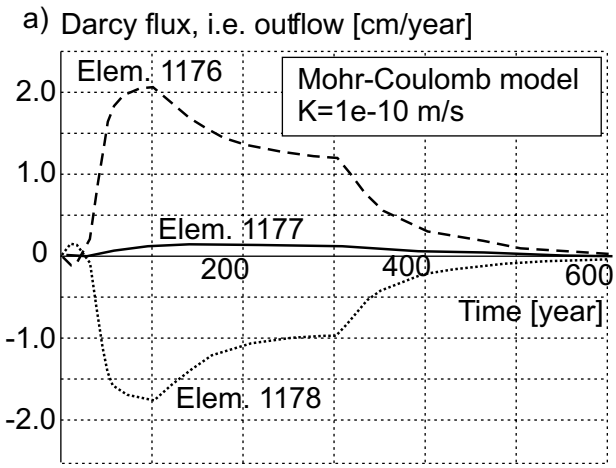

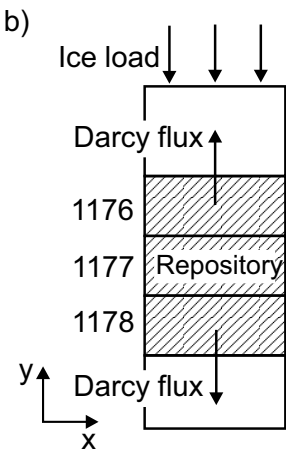

Fig. 8a. Vertical Darcy flux of the pore water through the Rupel Clay Member and the Asse Member clay (K = $1x10^{-10}$ m/s) during a moderately fast advance of the ice sheet, for a high lateral influx into the model. The clay is modelled by a Mohr-Coulomb material model. b. Sign convention and location of elements: 1178 = element at the bottom of the clay layer, 1177 = element in the middle of the clay layer and 1176 = element at the top of the clay layer.

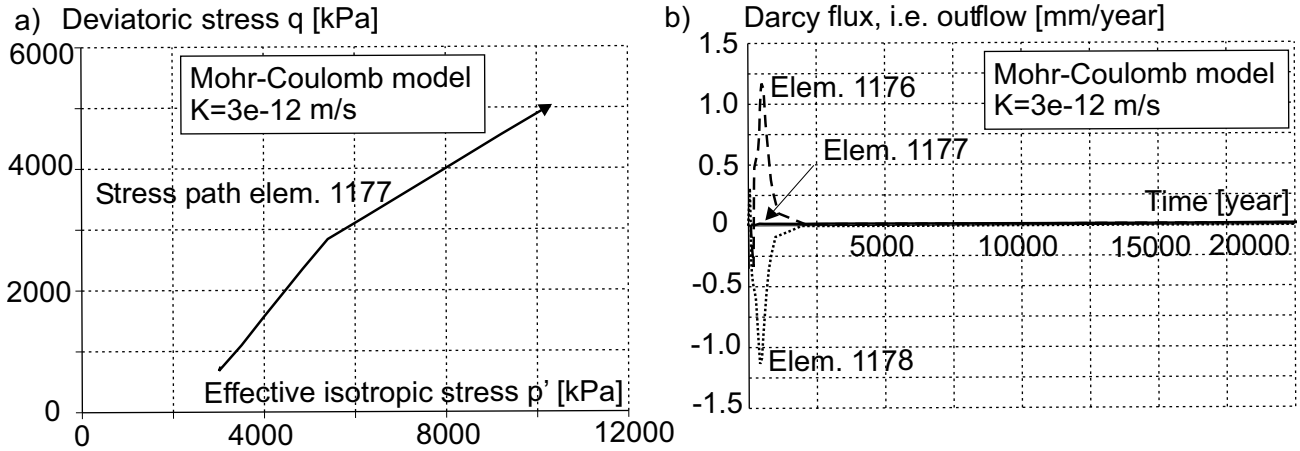

Fig. 9a. Evolution of the stress and b: the pore-water flow in the Rupel Clay Member and the Asse Member clay during glaciation. The clay is modelled by a Mohr-Coulomb material model. 1178 = element at the bottom of the clay layer, 1177 = element in the middle of the clay layer and 1176 = element at the top of the clay layer.

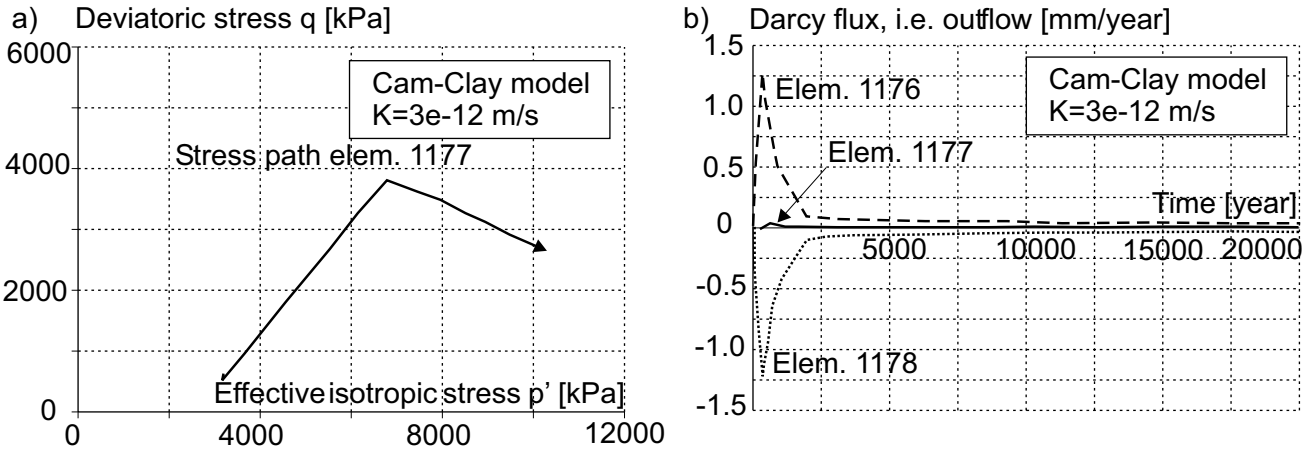

Fig. 10a. Evolution of the stress and b: the pore-water flow in the Rupel Clay Member and the Asse Member clay during glaciation. The clay is modelled by a Modified Cam-Clay material model.

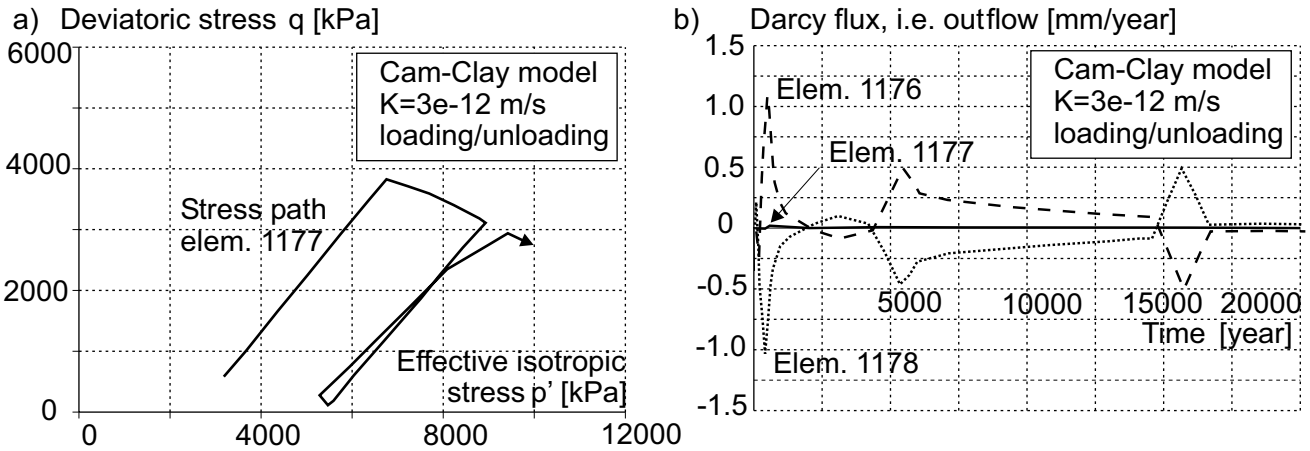

Fig. 11a. Evolution of the stress and b: the pore-water flow in the Rupel Clay Member and the Asse Member clay during glaciation. The clay is modelled by a Modified Cam-Clay material model. The model is loaded cyclically by the ice, with two loading and two unloading cycles.

due to unloading (Fig. 11a). Regardless of the material model used, the clay will, after initial elastic deformation, show plastic behaviour as a result of the ice loading. In particular, a low value for the friction angle ϕ will enhance plastic behaviour.

As a result of the ice loading, the Rupel Clay Member and the Asse Member clay consolidate, which causes vertical fluid flow within the clay (Figs 9b to 11b). The maximum outflow rate is similar in all the scenarios considered. For a realistic permeability val-

ue of $3x10^{-12}$ m/s the maximum outflow rate will increase to 1 mm per year at most. This is, approximately, three orders of magnitude higher than the flow rate in clay prior to ice loading of the model area.

The time needed for the clay to consolidate is very sensitive to its permeability and the assumed loading conditions. The use of the Modified Cam-Clay model for the clay in conditions of cyclic loading extends the duration of consolidation-driven flow. The flow rate exhibits a complex pattern, which generally follows the pattern of stress evolution (Fig. 11). During unloading, the clay swells, i.e., dilates. Swelling is accompanied by the suction-driven inflow of the pore water into the clay. This generally improves the isolation capacity of the clay, as the pore water flows inwards, towards the repository.

The flow rates in the aquifers will increase by approximately one order of magnitude compared to the situation before the ice loading. The increase in flow rates will more or less keep pace with the increase in stress caused by the ice loading. Once the maximum ice loading has been reached, the flow rate in the aquifer will decrease again rapidly.

Transport modelling

The impact of ice loading on radionuclide transport was evaluated by comparing it with radionuclide transport under the present-day conditions – i.e., the reference scenario. The results of the transport calculations, therefore, have only a relative significance. The METROPOL program was used to simulate transport of 17 radio-nuclides for a period of 1 million years (Sauter et al., 1993). The radionuclide source, the composition of which was taken from the METRO safety study (Grupa & Houkema, 2000), has been extrapolated for the Rupel Clay Member at a depth of 545 m. Eight decay chains, four of them comprising four members and five only one member, have been considered. It is assumed that radio-nuclides are released instantaneously, without delay, at the start of the simulation. Radionuclide transport occurs by the processes of diffusion, advection, dispersion and sorption of radio-nuclides to the clay (involving the retardation factor R). The natural rates of decay of radioactive materials have been taken into account.

A 10-km-long cross-section, which is part of the large-scale spatial model, was used for the transport calculations: This cross-section was subsequently extended into the third dimension, yielding a semi-three-dimensional model. The flow-rate range was calculated using the more detailed hydro-mechanical model, assuming a clay permeability of 3×10^{-12} m/s. Three representative velocity domains were generated; the present-day situation, and two glaciation situations, one with and one without an ice cover.

In modelling the radionuclide migration the three above models were used to calculate three different scenarios:

1. The present-day situation continuing for a further 1×10^6 years. This reference scenario and the present-day boundary conditions were used to calculate the relative mass fractions in scenarios 2 and 3, below.
2. Glacial conditions, i.e., a permafrost situation for a period of 1×10^6 years. This scenario and the associated glacial boundary conditions without an ice cover were used to evaluate the more realistic scenario 3, below.
3. Cyclic alternation of the present-day situation, lasting 6×10^4 years, a permafrost situation lasting 2×10^4 years and a glacial situation including an ice cover lasting 2×10^4 years. This sequence was repeated ten times covering a total duration of 1×10^6 years.

Under the influence of ice loading, fluid transport within the clay is also mainly diffusive. The orders of magnitude of the flow rates for the present-day situation and for the glacial situations with and without ice cover are respectively 10^{-7}, 2.5×10^{-7} and 1.7×10^{-5} m per year. These contribute for 0.08%, 0.2% and 14%, respectively to the total transport. These values apply if we assume a longitudinal dispersivity of 50 m.

In the aquifers above and below the clay, transport is strongly affected by flow, resulting in much faster migration of radio-nuclides. The reinforcing effect of the fault on radionuclide migration is clearly reflected in the pattern of the contour lines near the fault (Fig. 12). The effects of alternating climate conditions and in particular glacial conditions on the radionuclide mass fractions are shown in Fig. 13.

The glacial scenario without an ice cover results in lower mass fractions than the reference scenario. As a result of the higher flow rate in the overlying aquifer, the radio nuclides are rapidly diluted. Ice loading results in higher radionuclide mass fractions at the boundary between the clay and the overlying aquifer. Depending on which nuclide is considered, the mass fraction may be as much as two to nine times higher than in the reference scenario.

Conclusions

The presence of an advancing ice cap results in an increase in pore pressure in the deeper aquifers underneath that ice cap and in front of it. This may result in accelerated upward water flow through clay deposits

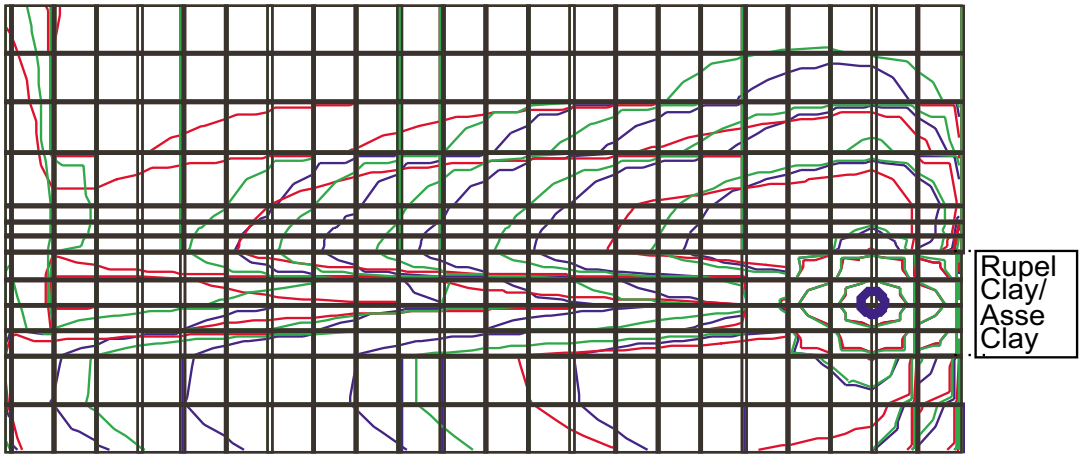

Fig. 12. Contours of mass fractions; blue = present-day conditions; red = permafrost conditions; green = cyclic alternation of present-day, glacial and ice-loading conditions. Relative levels are 1, $1x10^{-1}$, $1x10^{-2}$, $1x10^{-3}$, $1x10^{-4}$, $1x10^{-5}$, $1x10^{-6}$, $1x10^{-7}$, $1x10^{-8}$, $1x10^{-9}$. Fault is at the left side of the window.

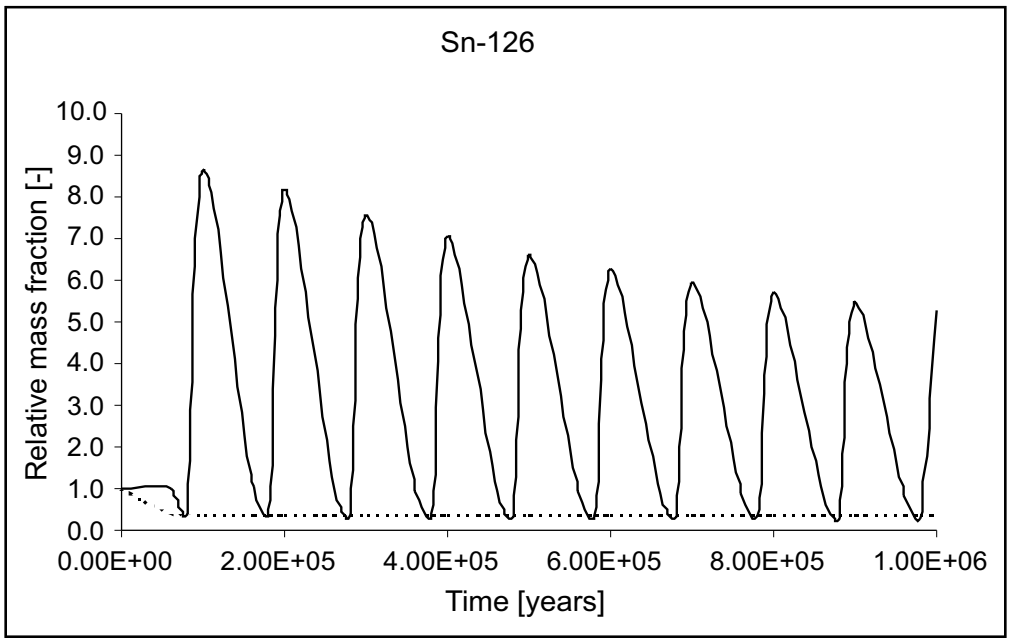

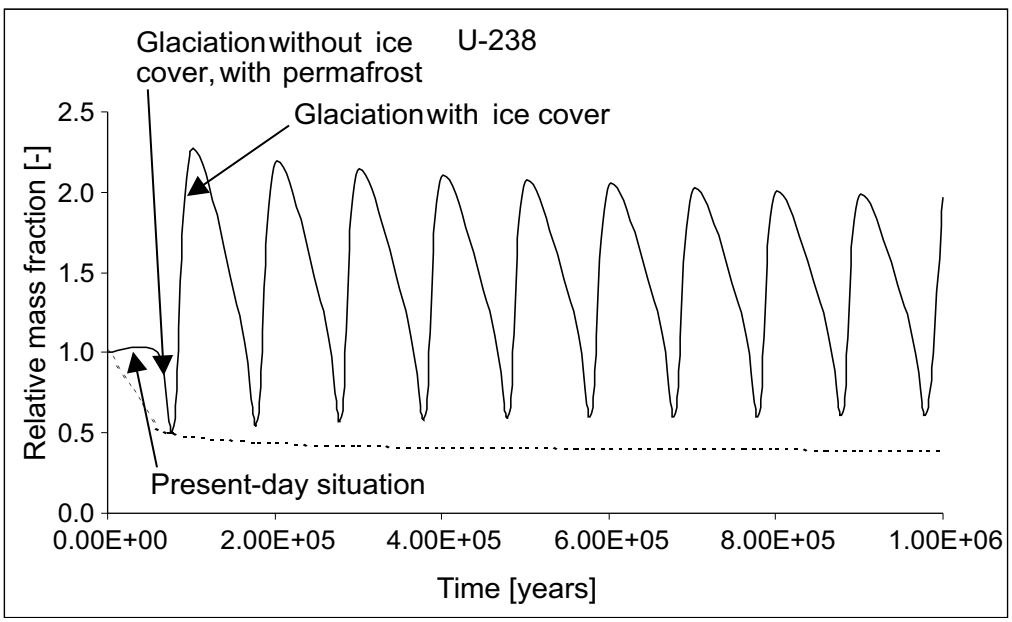

Fig. 13. Mass fractions of two radioisotopes at the boundary between the clay and the overlying aquifer in comparison to the present-day situation, i.e. the reference scenario; solid line = relative mass fraction for the scenario assuming cyclic changes; dashed line = relative mass fraction for the scenario assuming permafrost without an ice cover.

that have permeabilities equal to or exceeding 1×10^{-10} m/s. In a deeper clay section underneath an ice cap, water is expelled to both overlying and underlying water-bearing layers. Rates and durations of the consolidation-driven outflow are very sensitive to the permeability of the clay and the dynamics of loading by the ice. The consolidation of the Rupel Clay Member and the Asse Member clay may continue during the entire period of ice loading. The maximum outflow rate is 1 mm per year, which is approximately three orders of magnitude higher than the flow rate within the clay before ice loading.

The preliminary calculations indicate that the cyclic ice loading may result in accelerated radionuclide migration in clay. The contribution of dispersive transport to the total diffusion coefficient in clay amount to 0.08% under present-day conditions, 0.2% under glacial conditions without an ice cover, and 14% under glacial conditions with an ice cover. These values apply assuming that the longitudinal dispersivity is 50 m. In these percentages, sorption of radio-nuclides by clay is not taken into account. Cyclic ice loading with loading periods of 20,000 years over a total period of 100,000 years causes an increase in mass fractions of radio-nuclides at the boundaries of the clay barrier and the overlying aquifer. Depending on the particular radionuclide, this increase corresponds to a maximum of two to nine times the mass fraction in the reference scenario, i.e., continuation of the present-day climate. Such an increase is expected to be within the reliability interval of the estimated diffusive-transport rate. The calculations yielding the above values did take into account radionuclide sorption by clay.

At the time of the hydro-mechanical modelling most of the results from the experimental programme were not yet available. The lower experimental value for the effective pre-consolidation stress p'c and the higher experimental value for the compression index λ will eventually result in a slightly higher Darcy flux than found in the most realistic scenario presented here. The value used for the friction angle is higher than the values found in the experiments. In Cam-Clay models, a higher ϕ value is used to compensate for the cohesion parameter, since this parameter is not included in Cam-Clay models.

Acknowledgements

The financial support of the Ministry of Economic Affairs and the approval to perform the R&D work from the national Committee on Radioactive Waste Disposal (CORA Cie) are greatly appreciated. We are very grateful to B. Neerdael of SCK at Mol and A. Vervoort of Leuven University in Belgium for their support in providing and scanning of the clay samples, respectively. F. van Weert and Ms. C. Lehnen-de Rooij & E. den Haan from GeoDelft are thanked for their valuable contributions to the study. The fruitful discussions with H. Kooi and R. van Baalen both of the Free University of Amsterdam, G. Kruse of GeoDelft and J.P.A. Roest of the Technical University Delft during various stages of the project are very much appreciated. The grammatical improvements of Ms T. van de Graaff-Trouwborst (Thema Geologica) are highly acknowledged.

References

Bishop, A.W., Webb, D.L. & Lewin, P.I.,1965. Undisturbed samples of London Clay from the Ashford Common Shaft: strength-effective stress relationships. Géotechnique, 15: 1-31.

Boulton, G.S. & Curle, F., 1997. Simulation of the effects of long-term climatic changes on groundwater flow and the safety of geological disposal sites. University of Edinburgh, RIVM & RGD, European Commission, Nuclear Science and Technology, EUR 17793 EN.

Burland, J.B., 1990. On the compressibility and shear strength of natural clays. Géotechnique, 3: 327-378.

CORA Cie, 2001. Terugneembare berging, een begaanbaar pad? – Onderzoek naar de mogelijkheden van terugneembare berging van radioactief afval in Nederland: 110 pp.

DIANA 7.2, Program and User's Manuals, 2000. TNO Building and Construction Research.

Hageman, B.P. & Van de Vate, L. (in press). Retrievable disposal of radioactive waste in the Netherlands. In: Witherspoon, P.A. Geological problems in radioactive waste isolation – Third worldwide review, Chapter 20, LBNL.

Grupa, J.B. & Houkema, M., 2000. Terughaalbare opberging van radioactief afval in diepe zout- en kleiformaties. NRG, reportnr CORA 04.

Orlic, B. & Wildenborg, A.F.B., 2001. Simulation of glacially-driven hydro-mechanical processes for safety assessment of geological disposal sites. Annual Conference of the Int. Assoc. of Mathematical Geology (IAMG), Session M. CD-ROM. Cancun.

Sauter, F.J., Leijnse, A. & Beusen, A.H.W., 1993. METROPOL, User's guide. National Institute of Public Health and Environmental Protection, Bilthoven, RIVM Report 725205003.

Van Weert, F.H.A., Van Gijssel, K., Leijnse, A. & Boulton, G.S., 1997. The effects of the Pleistocene glaciations on the geo-hydrological system of Northwest Europe. Journal of Hydrology, 195: 137-159.

Wildenborg, A.F.B., Orlic, B., de Lange, G., de Leeuw, C.S., Zijl, W., Van Weert, F., Veling, E.J.M., de Cock, S., Thimus, J.F., Lehnen-de Rooij, C. & den Haan, E.J., 2000. Transport of Radio-nuclides disposed of in Clay of Tertiary Origin (TRACTOR). TNO-report NITG 00-223-B. Netherlands Institute of Applied Geoscience TNO – National Geological Survey.